

## C-8-2

Resistive switching memory using high- $\kappa$  Ta<sub>2</sub>O<sub>5</sub> films

Y.-R. Tsai<sup>1</sup>, S. Maikap<sup>1,4</sup>, D. Panda<sup>1</sup>, S. Z. Rahaman<sup>1</sup>, C. S. Lai<sup>1</sup>, P. J. Tzeng<sup>2</sup>, C. H. Lin<sup>2</sup>, T. C. Tien<sup>3</sup>, T.-Y. Wu<sup>2</sup>, C. C. Wang<sup>2</sup>, M.-J. Kao<sup>2</sup>, and M.-J. Tsai<sup>2</sup>

<sup>1</sup>Department of Electronic Engineering, Chang Gung University, Tao-Yuan, Taiwan.

<sup>2</sup>Electronics and Optoelectronics Research Laboratories, Industrial Technology Research Institute, Hsinchu, Taiwan

<sup>3</sup>Material Research Laboratories, Industrial Technology Research Institute, Hsinchu, Taiwan

<sup>4</sup>Corresponding author: Tel: 886-3-2118800 ext. 5785 Fax: 886-3-2118507 E-mail: [sidhu@mail.cgu.edu.tw](mailto:sidhu@mail.cgu.edu.tw)

### 1. Introduction

Many kinds of nonvolatile memory (NVM) devices with the technical limitations of scalability potential, higher switching power, nonvolatility, and reliability, etc have been reported by several groups [1-3]. To overcome those problems, a resistive switching memory device is one of the promising candidates for future nanoscale memories in the semiconductor industry. Different binary oxide memory elements such as NiO<sub>x</sub> [4], HfO<sub>x</sub> [5], Cu<sub>2</sub>O [6], etc have been reported by several groups. It is also expected that the flash memory device can be replaced by resistive switching memory in future. Recently, the resistive switching memory of the electrochemical formation and removal of metallic pathways in the GeSe solid electrolytes have been reported [7]. Due to the GeSe process limitation, the high- $\kappa$  solid electrolyte can be used for the nanoscale resistive switching memory applications. In this study, we have investigated the resistive switching memory in a Cu/Ta<sub>2</sub>O<sub>5</sub>/TiN/Si structure for the first time.

### 2. Experiment

A TiN metal with a thickness of ~60 nm for a bottom electrode was deposited by sputtering on 8 inch silicon (Si) substrate. Then, the high- $\kappa$  Ta<sub>2</sub>O<sub>5</sub> film with a thickness of ~15 nm was deposited by reactive sputtering using Ta target. The ratio of Ar and O<sub>2</sub> process gases was 1:1. The sputtering power and time were 100W and 10 min, respectively. Then, the Cu acted as a top electrode was deposited by thermal evaporation using shadow mask. The area of the top electrode was ~5x10<sup>-4</sup> cm<sup>2</sup>. A schematic memory structure of the Cu/Ta<sub>2</sub>O<sub>5</sub>/TiN is shown in Fig. 1. To probe the thickness and microstructure of the Ta<sub>2</sub>O<sub>5</sub> film, high resolution transmission electron microscopy (HRTEM) was performed. The thicknesses of the high- $\kappa$  Ta<sub>2</sub>O<sub>5</sub> and TiN metal layers are found to be ~15 nm and ~60 nm, respectively, for the as-deposited resistive memory devices as shown in Fig. 2. To drive the Cu into the high- $\kappa$  Ta<sub>2</sub>O<sub>5</sub> solid electrolyte, the post metal annealing treatment was performed. Electrical characteristics such as current-voltage (I-V), cycling and retention were performed using HP4156C semiconductor analyzer.

### 3. Results and discussion

Fig. 3 shows the x-ray photoelectron spectroscopy (XPS) characteristics of the as-deposited high- $\kappa$  Ta<sub>2</sub>O<sub>5</sub> films. The peak fitting is performed by Shirley background subtraction and Gaussian/Lorentzian functions. The peak binding energies of the Ta4f<sub>7/2</sub> and Ta4f<sub>5/2</sub> doublets are found to be 26.3 eV and 28.2 eV, respectively, which correspond to the Ta<sub>2</sub>O<sub>5</sub> films [8]. It is also observed that the peak binding energies of the Ta4f<sub>7/2</sub> and Ta4f<sub>5/2</sub> signals are found to be 21.7 eV and 23.6 eV, respectively, which correspond to the Ta metal. It means that high- $\kappa$  Ta<sub>2</sub>O<sub>5</sub> films contain small amount of Ta metal or Ta sub-oxide. After the annealing process, the peak binding energies of the Ta<sub>2</sub>O<sub>5</sub>4f<sub>7/2</sub> and Ta<sub>2</sub>O<sub>5</sub>4f<sub>5/2</sub>, and Ta4f<sub>7/2</sub> and Ta4f<sub>5/2</sub> signals are the same as shown in Fig. 4. The peak binding energies of the O1s spectra centered at 531.2 eV are also the same for the as-deposited and annealing of the Ta<sub>2</sub>O<sub>5</sub> films. The memory characteristics of our resistive switching devices in a Cu/Ta<sub>2</sub>O<sub>5</sub>/TiN structure after annealing treatment have been described. Current-voltage (I-V) and resistance-voltage (R-V) hysteresis characteristics have been shown in Figs. 6 & 7. The sweep is started from 0V to positive

bias 0.35 V (arrow 1) and the low current (high resistance: R<sub>high</sub>) can be switched to high current (low resistance: R<sub>low</sub>) limit (arrow 2). When the sweeping voltage is larger than the threshold voltage (V<sub>th</sub>=0.35V) then the resistive switching is observed. The maximum positive sweeping voltage of +1V can be applied for our memory device and the maximum current is limited by current compliance of 1mA. Now the memory device is sweeping back to +1V to 0V (arrows 3 & 4). The memory device can continue the low resistance state until the negative voltage of V<sub>e</sub>=-0.2V (arrow 5). After the negative voltage of -0.2V, the low resistance state is going to be high resistance state (arrow 6). A negative 1V is needed to become a high resistance state of the memory device and the device will maintain the high resistance state from -1V to +0.35V (arrow 7). If one can read the high resistance (R<sub>high</sub>=2x10<sup>5</sup> Ω) and low resistance (R<sub>low</sub>=4.4x10<sup>2</sup> Ω) states at a voltage of V<sub>read</sub> (=0.2V) then the ratio of R<sub>high</sub>/R<sub>low</sub> is 4.4x10<sup>2</sup>. The low resistance (R<sub>low</sub>) decreases with increasing the current compliance (not shown here). The ratio of R<sub>high</sub>/R<sub>low</sub> is high enough for application of multi-level charge (MLC) storage devices. A possible resistive switching mechanism is related to the electro-deposition and the electrochemical oxidation which can be seen in Fig. 8. By applying few hundred millivolts of positive bias on the Cu top electrode, the current (resistance) will increase (decrease) instantly due to the Cu ions diffusion from top electrode to the electrolyte. This electro-deposition process will lead the formation of metal bridge which can connect top and bottom electrode. However, when an opposite bias is applied on the top electrode, the metal bridge will break and the Cu ions will flow back to top electrode. This formation and rupture of the connection are due to the electro-migration and oxidation, respectively. The Cu diffusion is also confirmed by Arrhenius plot (Fig. 9). The activation energy of Cu ion diffusion is found to be 0.4 eV which is similar with the reported results [9]. Although the endurance of the resistive memory device is not good it can operate up to 4x10<sup>3</sup> cycles (Fig. 10). The retention characteristics are shown in Fig. 11. An initial R<sub>high</sub>/R<sub>low</sub> ratio is ~5.5x10<sup>2</sup> and it can have ~3.7x10<sup>2</sup> after 14 hours of retention at room temperature.

### 4. Conclusions

Novel resistive switching nonvolatile memory devices with low current of <1 mA, low voltage of <1V, high resistance ratio of >3.7x10<sup>2</sup> after 14 hours of retention in the Cu/Ta<sub>2</sub>O<sub>5</sub>/TiN structure, have been investigated. It is believed that the resistive memory devices can be useful in future nanoscale nonvolatile MLC applications.

### Acknowledgments

The authors are grateful to Prof. J.-R. Yang's group for their TEM support. This work is supported by Electronic and Opto-electronic Research Laboratories, Industrial Technology Research Institute (EOL/ITRI) under the contract no. GERPD260031.

### References

- [1] J. R. Hwang et al., IEDM Tech. Dig., 2005, p.161. [2] S. Maikap et al., Semicond. Sci. Technol., vol.22, p. 884, 2007. [3] S. Maikap et al., Appl. Phys. Lett., vol. 91, p. 043114, 2007. [4] I. G. Baek et al., IEDM Tech. Dig., p. 587, 2004. [5] H. Y. Lee et al., VLSI-TSA, p. 146, 2008. [6] A. Chen et al., IEDM Tech. Dig., p. 746, 2005. [7] M. Kund et al., IEDM Tech. Dig., p. 773, 2005. [8] A. Muto et al., Jpn. J. Appl. Phys., vol. 33, p. 2699, 1994. [9] T. Sakamoto et al., VLSI Tech. Dig., 38 (2007).

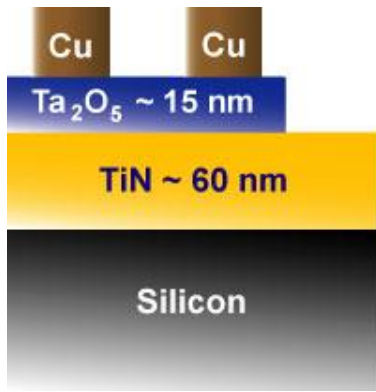


Fig. 1 Schematic of memory device using Cu/Ta<sub>2</sub>O<sub>5</sub>/TiN/silicon structure.

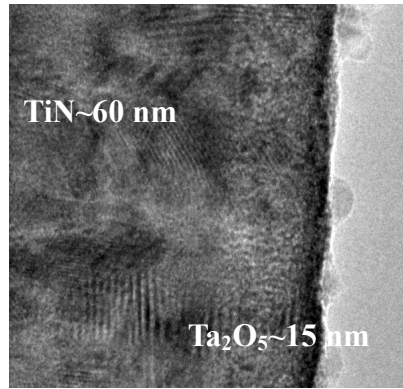


Fig. 2 Cross-sectional HRTEM image of as-deposited Ta<sub>2</sub>O<sub>5</sub> films on TiN as a bottom electrode.

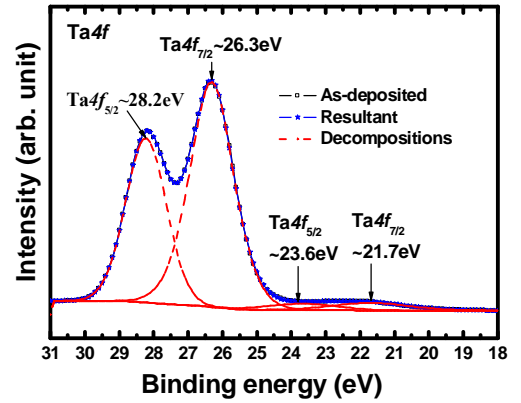


Fig. 3 Ta4f photoelectron spectra and peak decomposition results for the as-deposited Ta<sub>2</sub>O<sub>5</sub> films on TiN bottom electrode.

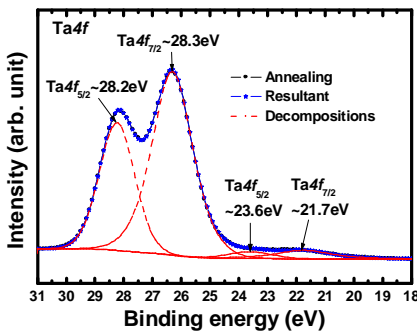


Fig. 4 XP spectra of Ta4f<sub>5/2</sub> and Ta4f<sub>7/2</sub> doublets and peak decomposition results for the annealed Ta<sub>2</sub>O<sub>5</sub> films.

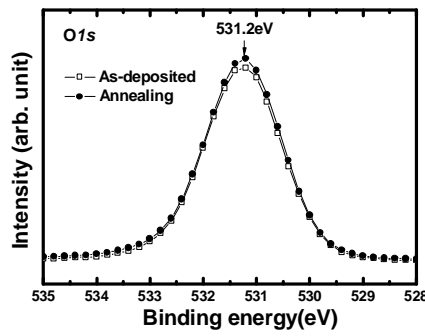


Fig. 5 O1s photoelectron spectra for as-deposited and annealed Ta<sub>2</sub>O<sub>5</sub> films.

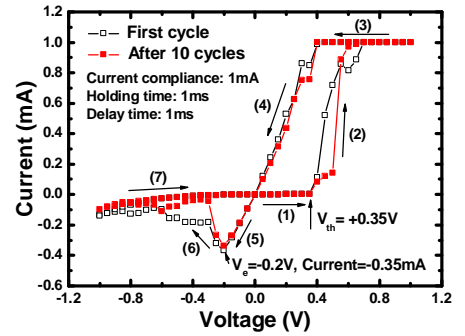


Fig. 6 I-V hysteresis of resistive switching memory in a Cu/Ta<sub>2</sub>O<sub>5</sub>/TiN/Si structure after annealing the device.

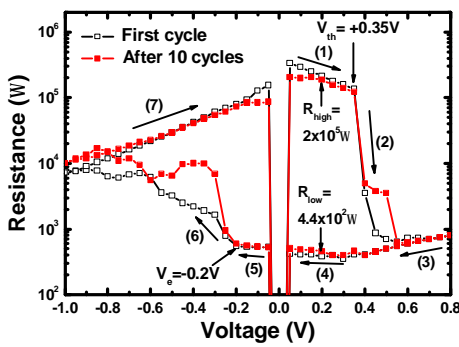


Fig. 7 Resistance versus applied voltage characteristics from Fig. 6.

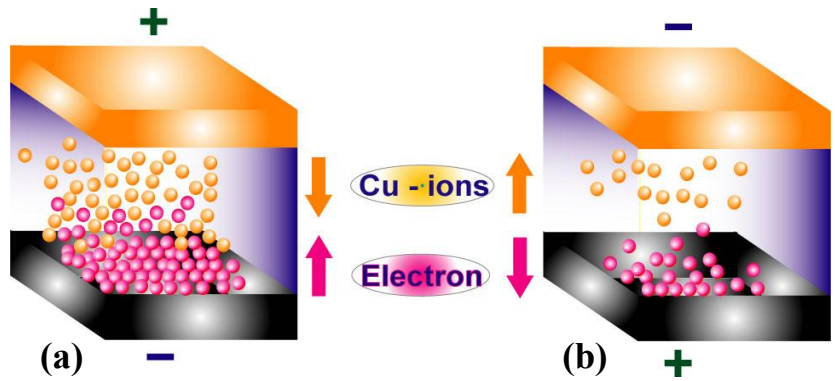


Fig. 8 Illustrations of switching mechanism with (a) positive and (b) negative bias applied on the top electrode.

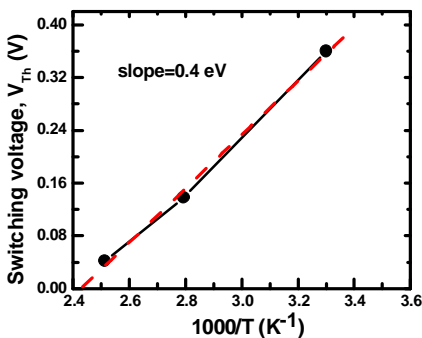


Fig. 9 Arrhenius plot for activation energy of Cu evaluation.

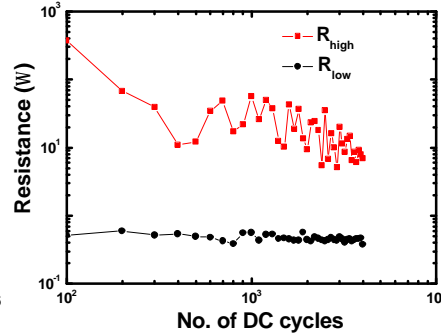


Fig. 10 Endurance characteristics of resistive switching memory devices with current compliance of 1mA.

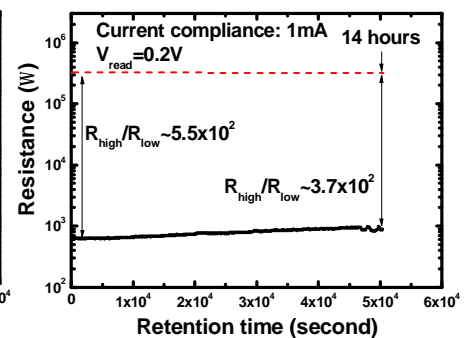


Fig. 11 Retention characteristics of the resistive switching memory devices at room temperature.